Journal of Ceramic Processing Research. Vol. 26, No. 1, pp. 162~171 (2025)
(Received 29 August 2024, Received in revised form 18 December 2024, Accepted 10 January 2025)
https://doi.org/10.36410/jcpr.2025.26.1.162

J O U R N A L O F
Ceramic Processing Research

Analysis of the arsenic adsorption and desorption in iron oxyhydroxides (ferrihydrite and goethite) in a dynamic system

T. Alejandro De la Peña, M. Adrián Zamorategui*, A. Oscar Coreño and O. Norma Leticia Gutiérrez
Department of Civil and Environmental Engineering, University of Guanajuato, 36000 Guanajuato, Mexico

Arsenic present in drinking water as a contaminant poses health risks. Iron oxyhydroxide granules were used as adsorbents to remove arsenic in a dynamic system in aqueous media. The granules were prepared with calcium alginate as a support medium. The results of the arsenic adsorption tests correspond to pseudo-first-order kinetics. The adsorption isotherms at various temperatures correspond perfectly to the Langmuir model. The thermodynamic parameters showed that the adsorption process is exothermic and spontaneous. The performance of a column packed with pellets to remove arsenic in an aqueous medium in a dynamic system was analyzed. The rupture curves showed arsenic adsorption capacities of approximately 30 mg/g for rupture times of 7 hours on average, agreeing with the experimental results with the Thomas model. Desorption tests for the recovery of removed arsenic showed the reusability of the column for up to three cycles.

Keywords: Adsorption, Desorption, Arsenic, Columns, Model Thomas.

Introduction

Worldwide, especially in Latin America and Mexico, there is a problem of arsenic contamination. A large part of the population drinks water with an arsenic concentration that exceeds the current regulations for drinking water, which puts their health at risk [1]. The World Health Organization (WHO) has investigated water quality and concluded that one out of every 10,000 people is at risk of drinking water contaminated with arsenic concentration than 0.01 mg/L of arsenic which may cause damage to kidneys, liver, cause skin cancer, and other cancer [2].

In Mexico, arsenic contamination of the environment is due to the use of pesticides, the thermoelectric industry, and mining, among others. Arsenic in aqueous solutions can be present in As^{3+} and As^{5+}, where As^{3+} is the most toxic type and is stable in acidic to neutral pH solutions [3, 4].

The methodologies used for arsenic removal in aqueous solution range from coagulation, flocculation, reverse osmosis, and electrochemical methods. However, the adsorption process has several advantages, especially if the adsorbents are affordable, and can be regenerated and reused [5].

It is important to select the proper adsorbent material and to know its maximum adsorption capacity, as well as its physicochemical behavior [6]. Adsorption can be a physicochemical phenomenon (reversible or irreversible) based on the nature of the forces and bonds between the adsorbing surface and the molecules that are adsorbed. It is mainly attributed to the interaction of iron oxyhydroxide groups with ions, atoms, or molecules, through various mechanisms, such as electron donor-receptor reactions and/or the formation of metal complexes on the surface of the oxide [7].

Some isotherm models (Langmuir, Freundlich, Temkin, and Dubinin-Radushkevich) have been studied to understand how the adsorbate interacts with the adsorbent and to prove the most suitable correlation for the equilibrium conditions in the adsorption process [8, 9].

Arsenic is often found naturally adsorbed on surfaces of iron oxyhydroxides, such as ferrihydrite and goethite [6, 10, 11], so it is important to use these types of materials for removal from aqueous solutions. When ferrihydrite precipitates, it becomes a suitable substrate for adsorbing soluble compounds, such as phosphates, arsenates, silicates, and organic and heavy metals [12] and, at the same time, it presents a highly reactive surface area (200-500 m^2/g) [13]. Due to its low solubility compared to goethite and jarosite, ferrihydrite is one of the most stable in aqueous systems [14]. Goethite has a higher adsorption affinity for arsenic (As^{5+}) independent of the pH process [15]. It is important to investigate supports to immobilize materials with adsorption capacity, such as alginates, silica-gel, and glutano aldehyde [16, 17], to efficiently perform adsorption, regeneration and reuse processes in continuous systems [18].

These types of systems can be fed in a descending or ascending order in a column, creating a mass transfer or mass exchange zone, where adsorption and

*Corresponding author:
Tel : +52-473-137 1216
Fax: +52-473-102-0100 ext. 5915
E-mail: zamorategui@ugto.mx

saturation of the column occur gradually, so that the inlet concentration (C) becomes equal to the outlet concentration (C0), resulting in an inflection point in the elution curve [7, 19]. The inflection point, which is known as the breakpoint, provides information on the parameters of packed column systems and represents the metal exit concentration (expressed as a dimensionless number C/C0 versus time) [20]. Some theoretical models can be used to predict adsorption curve profiles, as a form of application and scaling. One of the most widely used models is the Thomas model [21-23]. The main objective of this work is the modeling and validation testing of the analysis design, as well as the analysis of the performance of the alginate pellet-packed column with iron oxyhydroxides for arsenic removal from aqueous solutions in continuous systems.

Methodology

Preparation of agglomerates iron oxyhydroxides (ferrihydrite and goethite) with calcium alginate

Alginate has natural agglomeration properties in the presence of calcium and is used as support using adsorbent material.

Different mass ratios of alginate and oxyhydroxides were used to determine the alginate/oxyhydroxides ratio for the preparation of the agglomerates. Figure 1 shows the ratios of the mixtures used against the densities of the agglomerates obtained. The 1:2 ratio presented greater stability against fracture for an agglomerate density, due to the greater amount of oxyhydroxides.

On the other hand, the material becomes more soluble at lower densities corresponding to a higher presence of alginate. The shaping of the spherical pellets was carried out by using a drip system with a peristaltic pump, the alginate solution with iron oxyhydroxides is dripped into a 1 M $CaCl_2$ solution [24-26].

Arsenic adsorption kinetics on iron oxyhydroxide agglomerates (goethite and ferrihydrite) supported on calcium alginate

To 1 g samples of calcium alginate agglomerates with synthetic goethite or ferrihydrite, 35 ml of a 10.0 ppm arsenic standard solution at pH 4.5, prepared from sodium arsenite, were added in six different 60 ml polypropylene tubes, respectively. The tubes were kept in a water bath at 25 °C with constant agitation to promote the interaction of the solute and the solid, thus favoring the adsorption of arsenic. Adsorption was suspended by centrifuging each tube at different times up to 10 h. The remaining arsenic was calculated as arsenic in the tubes. The remaining arsenic was calculated in the supernatant by GH-EAA. Each of these experiments were performed in triplicate and the amount of adsorbed arsenic was calculated by difference from the control under the same conditions but without adsorbent [27].

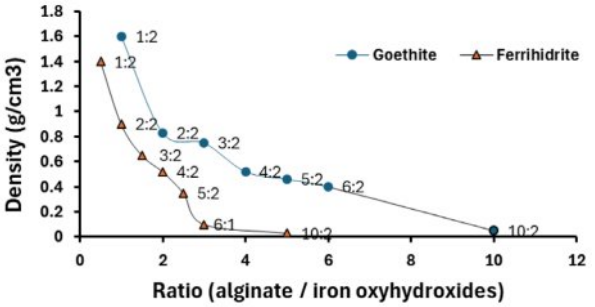

Fig. 1. Ratio of alginate to iron oxyhydroxides (ferrihydrite and goethite).

Arsenic adsorption isotherms, and their thermodynamic parameters at different temperature levels, on agglomerates of iron oxyhydroxides (goethite and ferrihydrite) supported in calcium alginate

Thirty-five ml of arsenic standard solution was added to 1 g samples of goethite or ferrihydrite. These solutions were prepared from sodium arsenite of different concentrations (0.1, 0.2, 0.5, 0.8, 1.2, 2.5 and 3 ppm) in seven different 50 ml polypropylene tubes, respectively. The tubes were kept in a water bath at 25 °C with constant agitation for 24 h to ensure equilibrium. After this time, adsorption was stopped by centrifuging each of the tubes; the remaining arsenic concentration was calculated in the supernatant by GH-EAA.

This procedure was repeated for 35 and 45 °C. Each of these experiments was performed in triplicate and the amount of arsenic adsorbed was calculated by difference with respect to the control under the same conditions, but without adsorbent.

Determination of thermodynamic parameters

The analysis of these parameters allowed for estimating the feasibility of the adsorption process, as did the effect of temperature on them. For this work, the following were estimated: standard Gibbs free energy (ΔG^o), standard enthalpy (ΔH^o) and standard entropy (ΔS^o) [2, 28].

Gibbs free energy allows discerning whether a process is spontaneous or not. Negative values of ΔG^o imply a spontaneous process, while positive values mean that it is necessary to contribute energy to the system, since it is not able to evolve by itself. It is calculated from equation (1):

$$\Delta G^o = -R \times T \times \ln Kc \quad (1)$$

This equation is used, in the first instance, at the level of ideal gas systems, but it can equally well be used for adsorption at very dilute solid-liquid interfaces, since this implies that the intermolecular distance is large enough to guarantee ideal gas-type behavior. Where R is the universal gas constant, T is the temperature in degrees Kelvin and K_C is the Langmuir constant.

The Vant Hoff equation allows obtaining graphically the values of ΔH^o and ΔS^o [2]. It is important to calculate it, as it provides information on the exothermic or endothermic nature of the process. In addition, it is also possible to estimate energy activation and differentiate whether it is a process occurring via physical (low values) or chemical adsorption (high values). This equation is obtained from the Gibbs free energy equation (2) as follows:

$$\Delta G^o = \Delta H^o - T \times \Delta S^o \quad (2)$$

Equating (1) and (2) gives:

$$-RTlnK_C = \Delta H^0 - T\Delta S^0 \quad (3)$$

Solving for ln K_C gives the Vant Hoff equation (4).

$$lnK_C = \frac{-\Delta H^0}{RT} + \frac{\Delta S^0}{R} \quad (4)$$

A graph of ln Kc on the abscissa axis and T^{-1} on the ordinate axis should be linear and the interception would equal $\Delta S^o/R$ while the slope would be numerically equal to $\Delta H^o/R$. For its part, K_C is figured out as follows [29]:

$$K_C = \frac{C_{Ae}}{C_{Se}} \quad (5)$$

C_{Ae} is the concentration of the adsorbate in equilibrium contained in the surface of the adsorbent and C_{Se} is the concentration in solution in equilibrium.

Adsorption enthalpy indicates whether the process is exothermic or endothermic and allows estimating the activation energy and differentiating whether it occurs by physical adsorption (low values) or chemical adsorption (high values). It is calculated by applying equation (6):

$$\Delta H^0 = \left[\frac{RT_1T_2}{(T_2 - T_1)}\right] ln\left(\frac{K_{C2}}{K_{C1}}\right) \quad (6)$$

Where: R is the ideal gas constant, K_{C1} and K_{C2} are the equilibrium constants at temperatures T_1 and T_2 respectively [30].

Adsorption entropy allows prediction of the size of changes on the adsorbent surface, as reversibility is affected therein, which would result in a negative value of adsorption entropy. Otherwise, it is indicative of a high possibility of reversibility.

Determination of the arsenic adsorption breakthrough curve vis a vis agglomerate of iron oxyhydroxides (goethite and ferrihydrite) supported in calcium alginate and of the Thomas model validation

Figure 2 shows the breakup curves obtained for the three different working heights (5, 10, and 14 cm), with a constant volumetric flow rate of 1 cm^3/min and a constant inlet concentration of 1 ppm arsenic. Under these conditions, the breakup time increased from 100 min to 2000 min for goethite and from 100 to 1800 min for ferrihydrite, indicating that, as the column height increases from 5 cm to 14 cm, the arsenic removal efficiency is higher.

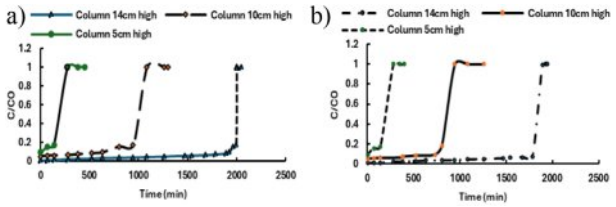

Fig. 2. Determination of optimum packing height a) goethite and b) ferrihydrite.

A slope change in the breakthrough curves is observed, being more vertical for the 14 cm column, indicating a larger transfer zone [31]. In addition, an increase in height implies an increase in adsorbent surface area. This leads to a longer operating time of the column, which allows a larger volume to be adsorbed.

The packed column can be calibrated according to the required contact time of the solution with the adsorbent. For this purpose, a 14 cm high packed column of alginate agglomerate with iron oxyhydroxides (ferrihydrite and goethite) with an internal diameter of 1.4 cm is used, whose internal flow of distilled water is controlled by a peristaltic pump and the minimum permissible flow rate is measured.

The service time of the packed columns is figured out by the breakthrough point. One column with an internal diameter of 1.4 cm and a packing height of 14 cm with an alginate agglomerate with iron oxyhydroxides (ferrihydrite and goethite) was used in this work. The absorption was performed in a continuous system with ascendant feeding using a peristaltic pump. The experimental results were compared with the Thomas model based on adsorption by the ionic exchange in a packed column [32, 33].

It is worth mentioning that the fits for the different models (BDST, Yoon-Nelson and Clark adsorption, and Thomas packed column) showed that the latter was the best fit. For the column design, the following mass balances were performed (Rafati et al., 2019). Material balance of the adsorbent bed [6].

$$C\dot{V}t_b^{id} = q_{\circ}m_A + C_0\varepsilon_B V_R, \quad (7)$$

Where:

$$[Ideal\ feed\ time] = [adsorbed\ amount] + \begin{bmatrix} amount\ of\ the\ liquid \\ phase\ within\ the\ voids\ of\ the\ bed \end{bmatrix}$$

Real material balance for the breakthrough curve

$$C_o\dot{V}\int_{t=0}^{t=\infty}\left(1 - \frac{C}{C_o}\right)dt = q_o m_A + C_o\varepsilon_B V_R, \quad (8)$$

$$[real\ feed\ time] = \begin{bmatrix} amount \\ adsorbed \end{bmatrix} + [storage\ capacity\ in\ the\ empty\ spaces]$$

Material balance differential

$$CapN_{accu} + N_{ads} = N_{disp} + N_{adv} \quad (9)$$

$$\begin{bmatrix} amount \\ accumulation \end{bmatrix} + \begin{bmatrix} amount \\ adsorbent \end{bmatrix} = \begin{bmatrix} output\ amount\ of \\ adsorbent \\ dispersion \end{bmatrix} + [output\ advection]$$

Thomas model
From the continuity equation (10).

$$\frac{\partial c}{\partial x} + \frac{\partial c}{\partial t} + \rho \frac{\partial q}{\varepsilon \partial t} = 0, \quad (10)$$

The initial and boundary conditions.

$$t = 0, x \geq 0, q = 0, \quad (11)$$

$$x = 0, t \geq 0, c = c_0, \quad (12)$$

The continuity equation solved by Thomas [34] is presented in equation (13). In this model, piston flow and negligible dispersion are considered.

$$Cap \frac{C}{C_0} = \frac{1}{1+\exp\left(\left(\frac{k}{Q}\right)(qhe - C_0 Ve)\right)}, \quad (13)$$

The equation (13) can be linearized in the form:

$$n\left(\frac{C_0}{C} - 1\right) = \frac{kqmc}{Q} - kC_0 t, \quad (14)$$

Where k is the Thomas constant, q is the adsorption ability, Q is volumetric flow, C_0 is the first concentration, and t is the time.

The difference between experimental value $(C/C_0)_e$ and theoretical value $(C/C_0)_m$, can be valued statically by the error equation (15).

$$CpRMSE = \sqrt{\frac{\left(\frac{C}{C0}\right)_m - \left(\frac{C}{C0}\right)_e}{n}}, \quad (15)$$

Where n is the data number, when experimental data and theoretical data are similar the RMSE decreases.

Recovery of adsorbed arsenic

In an arsenic adsorption system, agglomerates of iron oxyhydroxides (goethite and ferrihydrite) supported on calcium alginate are important to determine the desorption and readsorption capacity of arsenic. At least three cycles must be run to ascertain the useful service time. A glass column with an internal diameter of 1.4 cm and a 3 cm agglomerate packed height column were used in contact with 1 ppm and 3 ppm arsenic standard solution, respectively. After the adsorption processes, a $NaHCO_3$ solution is passed into the packed column with agglomerates of iron oxyhydroxides (goethite and ferrihydrite) supported on calcium alginate to carry out desorption. Subsequently, the adsorption and saturation technique is repeated two or more times necessary until the maximum reusability of the agglomerates is found.

The optimum $NaHCO_3$ concentration was 0.01 M, which allowed good desorption after at least two continuous cycles. Sodium bicarbonate in contact with calcium alginate, produces calcium carbonates, which weakens the calcium alginate structure. Therefore, the most effective concentration was 0.01 M.

The chemical reaction can be represented as follows:

$$Ca(C_6H_7O_6)_2 + 2NaHCO_3 \rightarrow CaCO_3 + 2Na(C_6H_7O_6) + H_2O + CO_2$$

Preparation of materials arsenic adsorbents with agglomerates of iron oxyhydroxides (goethite and ferrihydrite) supported in calcium alginate.

Agglomerates with an average diameter of 1.5 mm were obtained for ferrihydrite and 1.9 mm for goethite. This difference in diameter between the two iron oxyhydroxides is due to the fact that 80% of the ferrihydrite is obtained with a 140 mesh and 20% with an 80 mesh. However, the synthesized goethite is more irregular, with 75% obtained with an 80 mesh and the rest with a 60 mesh. A visual analysis of the morphology of the iron oxyhydroxide agglomerates supported on calcium alginate was carried out using a Quazar Qm 25 stereoscope.

In Fig. 3(a), the microscope with a 300x zoom is observed, showing the reddish amorphous crystals of ferrihydrite exposed on the calcium alginate support. Fig. 3(b) shows the brown amorphous crystals of goethite exposed to the calcium alginate agglomerate. In both cases, these are amorphous crystals, as reported by De la Peña et al. [27].

Figure 4 shows the SEM image of the iron oxyhydroxides: (a) shows the surface of ferrihydrite and (b) shows the surface of goethite, both with a resolution of 100 nm. As can be seen, ferrihydrite presents a smoother surface, because the crystals are less amorphous. On the other hand, in goethite, a rougher surface can be observed since the goethite crystal is more amorphous.

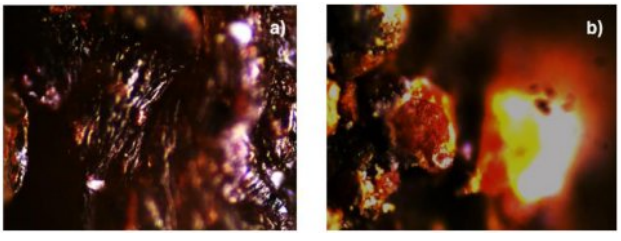

Fig. 3. shows the surface of the agglomerate of iron oxyhydroxide ferrihydrite (a) and goethite (b) supported in calcium alginate.

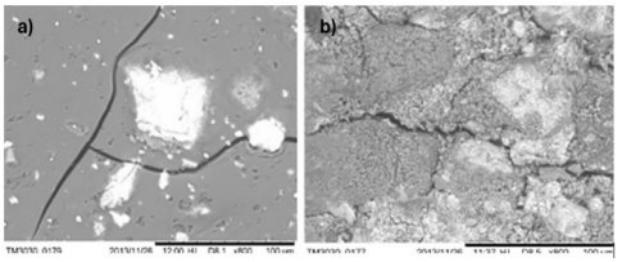

Fig. 4. SEM image of the surface of the calcium agglomerate: (a) ferrihydrite and (b) goethite.

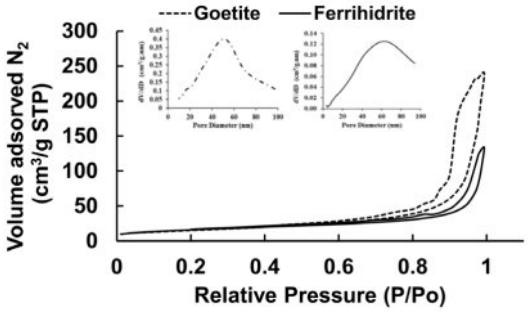

Fig. 5. BET isotherm and porous diameter of goethite and ferrihydrite.

However, in both cases carbonate formations or white spots can be observed on the surface of the materials, since iron oxyhydroxides tend to react with atmospheric oxygen [35] and cause these spots.

The adsorption-desorption isotherms of goethite and ferrihydrite agglomerates are shown in Fig. 5. According to the IUPAC classification, the BET isotherms are of type IV and correspond to mesoporous materials, with pores between 2 and 50 nm in diameter [36-40]. The BET surface areas obtained were 50.60 m^2/g and 54.30 m^2/g, and the pore diameter distributions obtained with the BJH adsorption model for goethite and ferrihydrite agglomerates were 50 nm and 60 nm respectively.

Arsenic adsorption kinetics on calcium alginate agglomerates with goethite and ferrihydrite.

Figure 6 shows that the arsenic adsorption equilibrium is reached in 30 y 40 min and that the adsorption capacity at this approximate time is 0.09-0.08 mg/g for the goethite (Fig, 6a) and ferrihydrite (Fig. 6b).

The values of arsenic adsorption kinetics were presented as the best fit to the pseudo-first-order model represented in equation (16). The adsorption processes using iron oxyhydroxides (goethite and ferrihydrite) at 25 °C at 10.0 ppm were fitted to the pseudo-first-order kinetic as shown in Fig. 7(a) and (b), proposing an ion exchange between the sorbate surface and the sorbent, as mentioned by Mahadeva and Colmenero [40, 44].

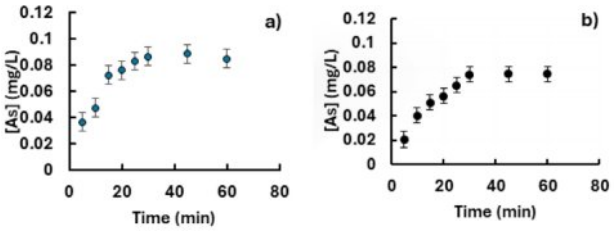

Fig. 6. Arsenic adsorption kinetics 10.0 ppm, 25 °C on agglomerates of calcium alginate with synthetic goethite (a) and ferrihydrite (b). Error bars are 95% confidence intervals.

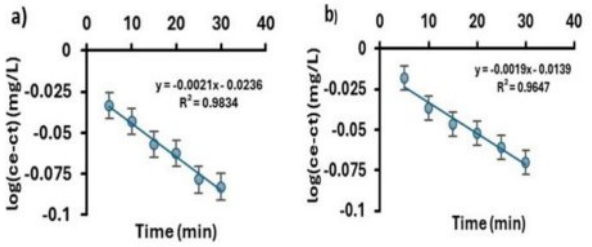

Fig. 7. Adjustment of the adsorption kinetics of arsenic 10.0 ppm, 25 ºC, on agglomerates of calcium alginate with synthetic goethite (a) and ferrihydrite (b), to the pseudo-first-order kinetic model. Error bars are 95% confidence intervals.

$$\log(C_e - C_t) = logC_e - \frac{k}{2.303}t \quad (16)$$

Where: C_e y C_t (ambos en mg/L) son las concentraciones As adsorbidos en el equilibrio y tiempo t (min), respectivamente, y k es la constante de velocidad. The slope gives us the system's adsorption rate constant, 0.0019 for ferrihydrite and 0.0021 for goethite, whose units are s^{-1} min^{-1}. This constant indicates the rate at which the concentration of the limiting reagent decreases. The parameters k and R are summarized in Table 1.

Table 1 shows the different kinetic models and their corresponding parameters for the process of adsorption of As. As shown, the best kinetic model fitted was the pseudo-first-order model. The pseudo-first-order model assumes that the adsorption rate is directly proportional to the concentration of adsorbate in solution. This means that the higher the adsorbate concentration, the higher the adsorption rate.

Table 1. Kinetics adjustment of the different theoretical models on agglomerates of calcium alginate with goethite.

	Ferrihydrite		Goethite	
Kinetics Models	K	R	K	R
Pseudo first order	0.0019	0.96	0.0021	0.98
Pseudo second order	0.83	0.51	0.81	0.5
ELOVICH	0.021	0.9	0.0022	0.86
Order n	0.0009	0.82	0.0004	0.41

Arsenic adsorption isotherms, and their thermodynamic parameters at different temperature levels, with agglomerates of iron oxyhydroxides (goethite and ferrihydrite) supported in calcium alginate

Figures 8 and 9 show the theoretical and experimental Langmuir isotherms for calcium agglomerates with goethite and ferrihydrite. The effect of temperature on the arsenic adsorption process is not temperature-dependent, since the concentration profile is practically the same at the different temperature levels tested, and the maximum arsenic adsorption on the synthetic materials is 26-30 mg/g at a temperature of 35 °C. The adsorption capacity of iron oxyhydroxide agglomerates (goethite and ferrihydrite) supported on calcium alginate is superior compared to the synthetic materials as reported by Cano R. [45], being 15 and 18 mg/g, this increase in adsorption may be due to the participation of calcium alginate in arsenic adsorption, as reported by Krok [46, 47]. It has an affinity for arsenic because its surface is covered by -OH groups, which allows ion exchange.

It is important to mention that the pH at the end of the arsenic adsorption experiments on ferrihydrite and goethite presented a variation from pH 4.5 to pH 8.1. This variation in pH suggests that the arsenic adsorption mechanism may be taking place through ion exchange of the OH group by AsO_3.

These results are consistent with another report inferring that, in the process of arsenic adsorption on iron oxyhydroxides, arsenate or arsenite anions can displace the hydroxyl group, taking its place and that the charge

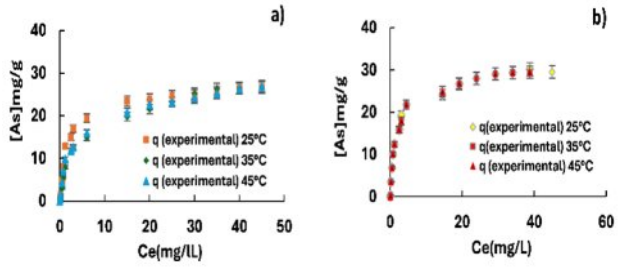

Fig. 8. Arsenic adsorption isotherms, at different concentrations and temperatures of 25,35 and 45 °C, on agglomerates of calcium alginate with synthetic goethite (a) and ferrihydrite (b). Error bars are 95% confidence intervals.

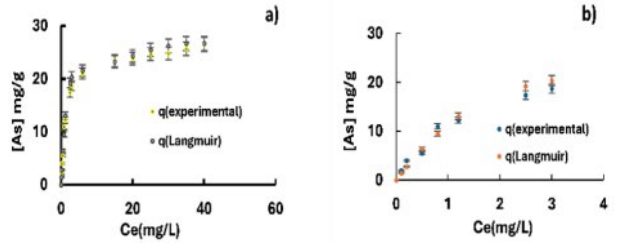

Fig. 9. The fit to the conventional Langmuir model shows the behavior of arsenic adsorption isotherms in calcium alginate agglomerates with goethite (a) and ferrihydrite (b).

Table 2. Isotherm adjustment of the different theoretical models on agglomerates of calcium alginate with goethite.

Adjustment of Theoretical Isotherms of Calcium Alginate Agglomerates with Goethite					
Isotherm	**K (l/mg)**	**N (mg/g)**	**n**	**R (J/molk)**	**R^2**
Langmuir	0.429	26.33		0.87	0.98
Freundlich	0.814		-0.473		0.65
Temkin	-1.069	566.87			0.75
D.R	-2.34E-08				0.81

Table 3. Isotherm adjustment of the different theoretical models on agglomerates of calcium alginate with ferrihydrite.

Adjustment of Theoretical Isotherms of Calcium Alginate Agglomerates with Ferrihydrite.					
Isotherm	**K (l/mg)**	**N(mg/g)**	**n**	**R (J/molk)**	**R^2**
Langmuir	0.533	30.44		0.87	0.99
Freundlich	0.883		-0.508		0.69
Temkin	-1560	-113			0.78
D.R	-2.47E-08				0.76

and size of the ions are factors determining adsorption by ion exchange [47].

It is important to mention that the adsorption of arsenic on goethite and ferrihydrite presented a better fit to the Langmuir isotherm model, with a 98% correlation for both materials. In addition, the higher theoretical adsorption capacity coincided with the experimental one. Other adsorption isotherm models evaluated showed very low fit correlations.

The tables show the fits to the different theoretical isotherms for both goethite (Table 2) and ferrihydrite (Table 3) agglomerates.

Determination of thermodynamic parameters

The standard Gibbs free energy is a thermodynamic parameter that allows for estimating the feasibility of an adsorption process. It allows us to discern whether a process is spontaneous or not. When the values of ΔG are negative, it is a spontaneous process, whereas, when they are positive, it is necessary to supply energy to the system, since it cannot evolve by itself. Using the molar weight of each contaminant, the Langmuir constant in the corresponding units (J/mol) was used to evaluate the

Table 4. Thermodynamic parameters calculated for agglomerates of calcium alginate with goethite.

Thermodynamic Parameters for Calcium Alginate Agglomerates with Goethite						
		units	25 C	35 C	45 C	R
Gibbs	ΔG	J/mol	-279.9	-458.3	-353.2	8.314
Entropy	ΔS	J/molK	-1.6	-2.0	-1.6	
Enthalpy	ΔH	J/mol	190.6	172.5	160.4	

Table 5. Thermodynamic parameters calculated for agglomerates of calcium alginate with ferrihydrite.

Thermodynamic Parameters for Calcium Alginate Agglomerates with Ferrihydrite						
		units	25 C	35 C	45 C	R
Gibbs	ΔG	J/mol	-255.9	-457.6	-356.1	8.4
Entropy	ΔS	J/molK	-2.5	-1.91	-2.18	
Enthalpy	ΔH	J/mol	501.5	430.5 1	337.1 6	

free energy. The calculated values of ΔG°, ΔH°, and ΔS° are summarized in Tables 4 and 5. As observed at the temperature of 35 °C the value of ΔG° is negatively larger, favoring the spontaneous reaction.

In the case of adsorption of calcium, alginate agglomerates with goethite, as well as for calcium alginate agglomerates with ferrihydrite, the values obtained allow interpreting the process as a spontaneous, exothermic phenomenon and the negative value of the entropy variation is characteristic of phenomena that go to a higher degree of order, such as adsorption. This value reflects a decrease in randomness at the adsorbent/solution interface during the process. The free energy value (ΔG°) is negative, indicating that the adsorption process is spontaneous. The enthalpy associated with the process is less than 10 kJ/mol; and suggests that it is an exothermic adsorption process [10, 48].

Determination of the arsenic adsorption breakthrough curve in terms of calcium alginate agglomerate with iron oxyhydroxides (ferrihydrite and goethite) and Thomas model validation

The minimum flow rate allowed in the peristaltic pump was 2 ml/min and by adding reflux in the pump feed, the flow rate was reduced to 1.5 ml/min.

Figures 10(a) and (b) show the breakthrough curves of arsenic adsorption at concentrations of 1 ppm and 3 ppm, respectively. The experimental and theoretical results correspond to the column packed with calcium alginate agglomerate with iron oxyhydroxides (ferrihydrite).

Using the least square method, the Thomas model with the linear equation shows a coefficient of fit (R^2) of 0.99.

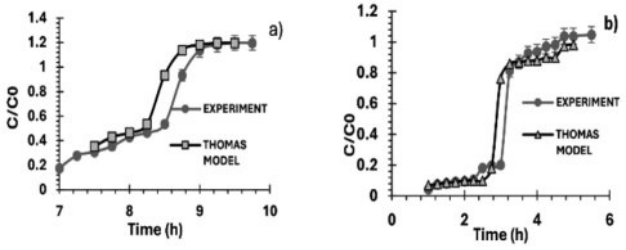

Fig. 10. Arsenic adsorption breakthrough curve in a packed column with calcium alginate agglomerate with ferrihydrite and comparing with the Thomas model, (a) C_0 = 1 ppm, (b) C_0 = 3 ppm.

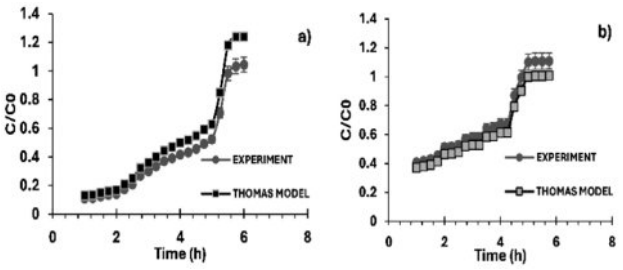

Fig. 11. Breakthrough curve adsorption (a) 1 ppm arsenic, (b) 3 ppm arsenic, in packed column with calcium alginate agglomerate with iron oxyhydroxides (goethite).

The breakpoints on the column loaded with 3.9 g of agglomerate and a concentration of 1 ppm were reached at 8 h 50 min. The breakpoints on the column with 3.7 g of agglomerate and a concentration of 3 ppm were reached at 3 h.

In the comparison between experimental and theoretical values, the error was RMSE = 0.16 for a concentration of 1 ppm and RMSE = 0.13 for a concentration of 3 ppm, indicating that the experimental and theoretical values are similar and corroborating the value of the correlation coefficient.

Figures 11(a) and (b) show the arsenic adsorption breakpoint at a concentration of 1 ppm and 3 ppm, respectively, both experimental and theoretical, of a column packed with calcium alginate agglomerate with iron oxyhydroxides (goethite).

The experimental data were fitted to the Thomas model by a linearized equation with a coefficient of fit (R^2) of 0.99, using the least square method. The column breakpoint time, at which an arsenic concentration of 1 ppm was reached, was achieved with a mass of 3.5 g of agglomerate and a packed height of 3 cm in a time of 5 h 30 min; the column breakpoint time, at which an arsenic concentration of 3 ppm was reached, was achieved with a mass of 3.7 g of agglomerate in a time of 4 h 15 min.

When comparing the experimental values with the theoretical values, it is observed that the RMSE error is 0.12 for a concentration of 1 ppm and 0.13 for a concentration of 3 ppm. This shows that both experimental and theoretical values are similar and corroborate the value of the correlation coefficient.

Recovery of arsenic adsorbed through two ways, using HCl 5% and 0.01 M $NaHCO_3$

By evaluating the difference between the arsenic concentration at the inlet and outlet of the column, it was determined that the adsorbed arsenic recovery process and the simultaneous regeneration of the adsorbent were carried out through a 5% HCl solution in a continuous system.

Figure 12 shows the calcium alginate agglomerates with iron oxyhydroxides (ferrihydrite) in contact with a standard solution (a) of 1 ppm and (b) of 3 ppm of

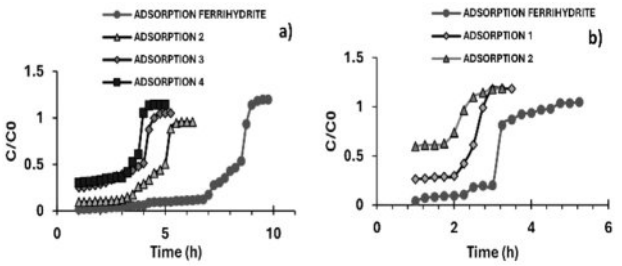

Fig. 12. Cycles of arsenic adsorption (a) C_0 = 1 ppm and (b) C_0 = 3 ppm, in calcium alginate agglomerates with iron oxyhydroxides (ferrihydrite) in a column 3 cm high.

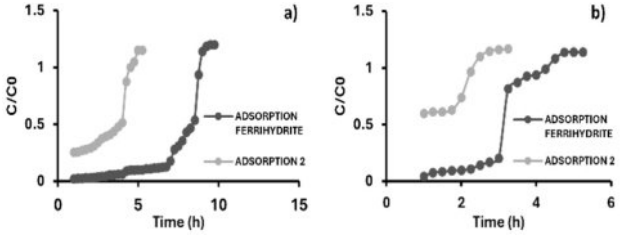

Fig. 14. Breakthrough curves of the arsenic adsorption cycles. Inlet concentration of (a) 1 ppm, (b) 3 ppm, calcium alginate agglomerate with iron oxyhydroxides (ferrihydrite).

arsenic, which can be reused at least four times in an adsorption-desorption process, since after the fourth cycle, the column goes out of service due to a 30% decrease in its adsorption capacity.

The reduction process of HCl in contact with ferrihydrite causes a decrease in adsorption capacity. This results in the corrosion of the agglomerate surface and the formation of iron(II) chloride, which is highly soluble and is released during washing [10], leading to changes and losses in the adsorbent material.

The corrosion process that the material undergoes is physically visible since the measured diameters of the agglomerates decrease by 30%, which results in a decrease in the arsenic adsorption capacity. Using 5% HCl may establish an unviable adsorbent agent due to the damage caused to the adsorbent material. However, it is proposed as an adsorbent agent in the study of the use of carbonates, since in previous works by De la Peña et al. and Cano-Rodríguez et al. [27, 45] it was demonstrated that iron oxyhydroxides in the presence of carbonates follow an arsenic desorption process in the material.

Figure 13 shows that calcium alginate agglomerated with iron oxyhydroxides (goethite) in contact with a standard solution of (a) 1 ppm and (b) 3 ppm arsenic can be reused in at least three cycles of the adsorption and desorption processes, with the fourth cycle being spent and unusable.

It is worth mentioning that this material presents a similar phenomenon to the one described above, but, as goethite is more amorphous when it comes into contact with the oxygen environment, it enters into an accelerated oxidation process and forms an oxide layer that affects its adsorption capacity before being subjected to the dynamic system. The corrosion process that the material undergoes is physically visible and, when measured, it has been observed that the agglomerates have decreased in diameter by 50%, resulting in a decrease in adsorption capacity. This will result in less aggressive agents to desorb and efficiently regenerate the adsorbent.

Figure 14 shows the calcium alginate agglomerate with iron oxyhydroxides (ferrihydrite) (a) after arsenic adsorption and (b) the agglomerate after the arsenic desorption process with $NaHCO_3$.

It is proposed to use $NaHCO_3$, where the adsorbed arsenic recovery process and simultaneous regeneration with the adsorbent were performed using a 0.01 M $NaHCO_3$ solution in a continuous system.

It has been determined that the calcium alginate agglomerate with iron oxyhydroxides (ferrihydrite) in contact with a standard solution (a) of 1 ppm and (b) of 3 ppm arsenic can be reused for at least two cycles in an adsorption-desorption process since after the second cycle the column is out of service. This is due to a decrease in adsorption capacity of 30%.

This decrease can be explained because HCO^{3-} comes into contact with ferrihydrite and undergoes an ion exchange process between arsenate/arsenite ions, releasing them into solution [17]. However, the HCO^{3-} anion interacts with the calcium alginate and uncovers the ferrihydrite in the capsule through the alginate. This allows a second adsorption of arsenic. The use of

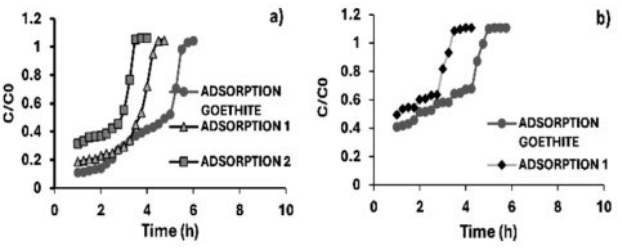

Fig. 13. Arsenic adsorption and desorption (a) 1 ppm and (b) 3 ppm in calcium alginate agglomerated iron oxyhydroxides (goethite).

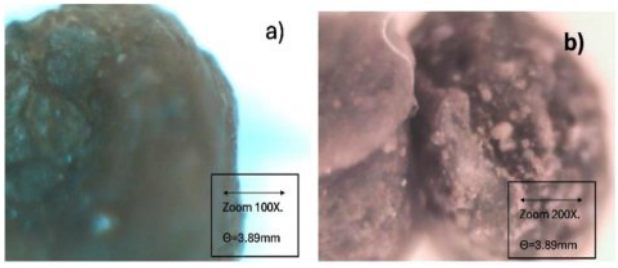

Fig. 15. (a) Ferrihydrite agglomerate with arsenic adsorbent before desorption with $NaHCO_3$, (b) Ferrihydrite agglomerate with arsenic adsorption/desorption after $NaHCO_3$.

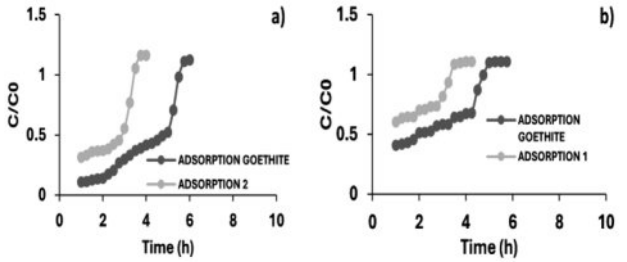

Fig. 16. Breakthrough curves of the arsenic adsorption and desorption cycles (a) 1 ppm, (b) 3 ppm in calcium alginate with iron oxyhydroxides (goethite).

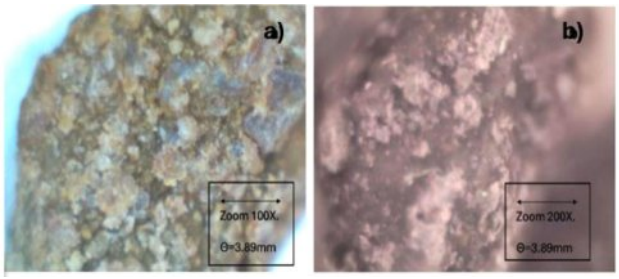

Fig. 17. (a) Goethite agglomerate with arsenic adsorbent before desorption with $NaHCO_3$, (b) Goethite agglomerate with arsenic adsorption/desorption after $NaHCO_3$.

$NaHCO_3$ can be established as an adsorbing agent.

Figure 15 shows the arsenic agglomerate with calcium alginate and iron oxyhydroxides (ferrihydrite) (a) before the desorption process with $NaHCO_3$ and (b) after the desorption process. The agglomerates show more cracking, with more material exposed.

It has been shown that the calcium alginate agglomerate with iron oxyhydroxides (goethite) with a standard solution (a) of 1 ppm and (b) of 3 ppm arsenic can be reused in at least two cycles of the adsorption and desorption process since after the third cycle the column becomes ineffective due to a 20% decrease in its adsorption capacity. The penetration curves for each cycle are shown in Fig. 16.

This material exhibits a similar phenomenon to that described above. However, goethite is more amorphous. In contact with ambient oxygen, it undergoes an accelerated oxidation process, forming an oxide layer that affects its adsorption capacity before the dynamic system.

Figure 17 shows an arsenic agglomerate with calcium alginate, and iron oxyhydroxides (goethite) before (a) and after (b) the desorption process with $NaHCO_3$. Figure 13 shows that the agglomerates show higher cracking and thus higher material exposure.

It is thought that the possible exposure of iron oxyhydroxides (for both ferrihydrite and goethite) is caused by the continuous flow of water creating a slight wear on the surface of the agglomerates.

Conclusion

The adsorption process of iron oxyhydroxides (goethite and ferrihydrite) is unaffected significantly by temperature changes. The correlation of the equilibrium data was fitted to the Langmuir adsorption isotherm and the adsorption process followed a pseudo-first-order kinetic model, which is related to chemical adsorption on the material surface. Ferrihydrite presented a higher As removal capacity (30 mg/g) compared to that obtained using goethite (26 mg/g).

Negative values of the variation of the free energy (ΔG) and a positive value of the enthalpy indicate that the adsorption process is spontaneous and exothermic. In addition, the negative value of the entropy variation is typical of phenomena that exhibit a higher degree of order and reflects a decrease in randomness at the adsorbent/solution interface during the adsorption process. The correlation of the experimental data fits the Thomas model, with ferrihydrite having a higher breakthrough point (8 hours) than goethite (5 hours).

The use of $NaHCO_3$ was the best option for the arsenic recovery process, as it did not damage the agglomerate structure compared to using HCl as a washing system The results obtained suggest that iron oxyhydroxide agglomerates, especially ferrihydrite, are promising materials for arsenic removal from water, offering an efficient and sustainable alternative to conventional methods.

Nomenclature

C	Concentration.
$\dot{V}$	Volumetric flow rate.
t_b^{id}	Real breakthrough time.
q_0	Equilibrium loading.
m_A	Mass.
ε_B	Bed porosity.
VR	Adsorber volume.
ΔG^o	Gibbs free energy.
R	Universal gas constant.
T	Temperature in Kelvin.
K_C	Langmuir constant.
ΔH^0	Standard enthalpy.
ΔS^0	Standard entropy.
C_{Ae}	The concentration of the adsorbate in equilibrium.
C_{Se}	Concentration in solution in equilibrium.
K_{C1} and K_{C2}	Equilibrium constants at temperatures.
k	Thomas constant.
Q	Volumetric flow.
t	Time.
C_0	First concentration.
q	Capacity adsorption.

m	Mass.
K	Langmuir, Freundlich, Temkin & D.R., constant.
N	Maximum adsorption ability.
n	Freundlich Constant.
r	D.R. constant.
R^2	Statical adjustment.

References

1. S.H. Frisbie and E.J. Mitchell, PLoS ONE. 17[4] 2022.
2. M. Shen, H. Guo, Y. Jia, Y. Cao, and D. Zhang, Appl. Geochem. [89] (2018) 190-201.
3. P.B. Penteado, D.C. Nogarotto, J.P. Baltazar, S.A. Pozza, and F.B. Canteras, CATENA 210 (2022) 105946.
4. Z. Qiu, X. He, F. Qiu, D. Yang, G. Yao, and T. Zhang, Sep. Purif. Technol. 250 (2020) 117165.
5. R. Somayeh, T. Mahamoud, K. Razieh, and A. Shahin, Appl. Water Sci. [9] (2019) 87.
6. L. Rafati, M.H. Ehrampoush, A.A. Rafati, M. Mokhtari, and A.H. Mahvi, J. Environ. Health Sci. Engineer 17 (2019) 753-762.
7. R. Wang, R. Liang, T. Dai, J. Chen, X. Shuai, and C. Liu, Trends Food Sci. Technol. [91] (2019) 319-329.
8. D. Balarak, F. Mostafapour, H. Azarpira, and J. Joghataei, Pharm. Res. Int. 20[2] (2017) 1-9.
9. B. Li, L. Yang, C.-Q. Wang, Q.-P. Zhang, Q.-C. Liu, Y.-D. Li, and R. Xiao, Chemosphere [175] (2017) 332-340.
10. B.A. Méndez-Ortiz, A. Carrillo-Chavez, and M.G. Monroy-Fernandez, Rev. Mex. Cienc. Geol. 24[2] (2007) 161-169.
11. A.O. Fariña, R. Gago, J. Antelo, F. Juan, S. Fiol, and F. Arce, Bol. Soc. Geol. Mex. 67[3] (2015) 493-508.
12. J.L. Jambor, in "The relationship of mineralogy to acid-and neutralization-potential values in ARD" (Mineralogical Society of Great Britain and Ireland eBooks, 2000) 19-58.
13. D.G. Strawn, Soil Systems 5[1] (2021) 13.
14. E. Worch, in "Adsorption technology in water treatment" (De Gruyter eBooks, 2012).
15. C. Stamer and K. Nielsen, Water Supply 18[1] (2000) 625-627.
16. A. González-Martínez, M. De Simón-Martín, R. López, R. Táboas-Fernández, and B. Sánchez, Sustainability 11[12] (2019) 3307.
17. Y. Xu, S. Song, J. Chen, R. Chi, and J. Yu, J. Taiwan Inst. Chem. Eng. [99] (2019) 132-141.
18. D. Montalvo and E. Smolders, Vadose Zone J. 18[1] (2019) 1-9.
19. S. Ahmed, K. Hossain, W. Bruckard, N. Haque, and M. Chen, CSIRO. Australia and BCSIR Bangladesh (2021) 49-51.
20. A. Rasool, S. Muhammad, M. Shafeeque, I. Ahmad, F.A. Al-Misned, H.A. El-Serehy, S. Ali, B.A. Murtaza, and A. Sarwar, Hum. Ecol. Risk Assess. Int. J. 27[6] (2021) 1655-1670.
21. P. Kumkum and S. Kumar, J. Health Pollut. 10[28] (2020).
22. H. Patel, Int. J. Environ. Sci. Technol. 19[10] (2022) 10409-10426.
23. C. Sukumar, V. Janaki, K. Vijayaraghavan, S. Kamala-Kannan, and K. Shanthi, Clean Technol. Environ. Policy [19] (2017) 251-258.
24. S. Rawat and A. Maiti, Sep. Purif. Technol. 272 (2021) 118983.
25. N.T.T. Uyen, Z.A.A. Hamid, N.X.T. Tram, and N. Ahmad, Int. J. Biol. Macromol. [153] (2020) 1035-1046.
26. K.G. Gareev. Magnetochemistry 9[5] (2023) 119.
27. A. De la Peña-Torres, I. Cano-Rodríguez, A.F. Aguilera-Alvarado, Z. Gamiño-Arroyo, F. I. Gómez-Castro, M.P. Gutiérrez-Valtierra, and S. Soriano-Pérez, Rev. Mex. Ing. Quím. 11[3] (2012) 495-503.
28. N. Esfandiar, R. Suri, and E.R. McKenzie, J. Hazard. Mater. 423 (2022) 126938.
29. M.J. Amiri, J. Abedi-Koupai, S.M.J. Jalali, and S.F. Mousavi, J. Environ. Eng. 143[9] (2017) 04017061.
30. M.N. Sahmoune, Environ. Chem. Lett. 17[2] (2019) 697-704.
31. G.C. Castellar Ortega, B.M. Cardozo Arrieta, J.F. Suarez Guerrero, and J.E. Vega Taboada, Prospect. 11[1] (2013) 66-75.
32. J.B. Dima, M. Ferrari, and N. Zaritzky, Ind. Eng. Chem. Res. 59[34] (2020) 15378-15386.
33. M. Yusuf, K. Song, and L. Li, Colloids Surf. A. 585[20] (2020) 1-3.
34. A. Valencia, J. Kilner, N.B. Chang, and M.P. Wanielista, Water, Air, and Soil. [230] (2019) 1-28.
35. J.J.G. Martínez, en Efecto del Mn en el hábito cristalino de los (oxi) hidróxidos de hierro anclados en carbón activado: adsorción de As (V), Tesis, (Repositorio IPICYT, 2016).
36. R.K. Singha, A. Algahtanib, T. Al-Mughanamc, I. Mahdid and V. Tirthe, J. Ceram. Process. Res. 24[3] (2023) 525-534.
37. J. Rohana, D. Thenmuhilb, R. Umapriyac, and D. Varatharajanc, J. Ceram. Process. Res. 23[1] (2022) 22-28.
38. J. Llorente, C. Ramírez, and M. Belmonte, Wear 430 (2019) 183-190.
39. L.H.C. Sujo and M. de L. Villalba, Tecnoc. Chih. 17[3] (2023) 1261-1262.
40. J.W. Jeonga, K.J. Honga, J.J. Banga, K.J. Leea, K.A. Jeonga, T.S. Jeongb, and C.J. Younb, J. Ceram. Process. Res. 18[6] (2017) 463-470
41. B. Bendjus, U. Cikalova, and L. Chen. J. Ceram. Sci. Tech. 8[01] (2017) 73-80.
42. Z. Tong, Z. Shaofeng, F. Guangsheng, and M. Yuanhang, J. Ceram. Process. Res. 23[6] (2022) 845-852.
43. D. Suastiyantia, M. Wijayab, and B.G. Pandita, J. Ceram. Process. Res. 25[2] (2024) 261-267.
44. M.M. Swamy and B.M. Nagabhushana, in "Adsorption and its applications: Batch, Isotherms and Kinetic studies Clear the world from Pollution" (Sciencia Scripts. 2020) 25-28.
45. M.I. Cano-Rodríguez, A. De la Peña-Torres, B. Huerta-Rosas, A.F. Aguilera-Alvarado, Z. Gamiño-Arroyo, F.I. Gómez-Castro, and S.H. Soriano-Pérez, Amb. Techn. Sci. Mex. 3[1] (2015) 27.
46. B. Krok, S. Mohammadian, H.M. Noll, C. Surau, S. Markwort, A. Fritzsche, and R.U. Meckenstock. Sci. Total Environ, 807 (2022) 151066.
47. N. Seco-Reigosa, L. Cutillas-Barreiro, J.C. Nóvoa-Muñoz, M. Arias-Estévez, E. Álvarez-Rodríguez, M.J. Fernández-Sanjurjo, and A. Núñez-Delgado, Solid Earth 6[1] (2015) 337-346.
48. M.P. Murugesan, P. Akilamudhan, R.M. Venkata, K. Kannan, and V. Padmapriya, J. Ceram. Process. Res. 23[1] (2022) 90-98.